MOS Capacitance–Voltage Characteristics:
IV. Trapping Capacitance from 3-Charge-State Impurities*

Jie Binbin(揭斌斌)[1, 2, †] and Sah Chihtang(薩支唐)[1, 2, †]

[1]Department of Physics, Xiamen University, Xiamen 361005, China
[2]CTSAH Associates, Gainesville, Florida 32605, USA

Abstract: Metal–Oxide–Semiconductor Capacitance–Voltage (MOSCV) characteristics containing giant carrier trapping capacitances from 3-charge-state or 2-energy-level impurities are presented for not-doped, n-doped, p-doped and compensated silicon containing the double-donor sulfur and iron, the double-acceptor zinc, and the amphoteric or one-donor and one-acceptor gold and silver impurities. These impurities provide giant trapping capacitances at trapping energies from 200 to 800 meV (50 to 200 THz and 6 to 1.5 μm), which suggest potential sub-millimeter, far-infrared and spin electronics applications.

1. Introduction

The low-frequency and high-frequency capacitance-voltage (LFCV, HFCV) characteristics of the Metal–Oxide–Silicon (MOS) diode structures were theoretically and comprehensively investigated and reported by the senior author, Sah, in the early 1960's[1]. The effects from the dopant impurities in the Si substrate on the low-frequency capacitance were analyzed. Impurities described in Ref. [1] included the 1-energy-level acceptor and donor impurities without excited states, and the 2-energy-level or 3-charge-state impurities. Due to computation limited by slide-rule[2, 3], these 1960 theoretical studies[1] were limited to a few samples.

Our interest in the MOS capacitance–voltage characteristics was renewed recently[2], due to potential applications of the giant capacitance from trapping of electrons and holes at the donor and acceptor impurities, because these impurities are incorporated at high concentrations in the device structures of Metal–Oxide–Silicon capacitors (MOSCs) and transistors (MOSTs) of nanometer Si MOS integrated circuits. Using exact Fermi–Dirac distribution for the band electrons and holes, and the impurity occupation factor for the electrons and holes trapped at the single-energy-level donor impurity centers in our first computations, reported in Ref. [2], the LFCV and HFCV were numerically computed for MOSCs on n-type Si (n-MOSCs) with Phosphorus as the donor impurity. This was followed in our second[3] and third[4] reports, by varying the trap or bound-state energy level parameters of the 1-energy-level 2-charge-state impurities to delineate the parameters that produce the largest trapping capacitances[3] and also to characterize the common donor and acceptor dopant impurities in silicon and germanium semiconductors[4] for possible signal processing applications. In this fourth paper, we report the unique features that are present in the MOSCV characteristics from electron and hole trapping at the 2-energy-level 3-charge-state

donor, acceptor and amphoteric impurities, modeled for sulfur, iron, zinc, gold and silver in silicon. A special feature is noted, in indirect energy gap semiconductors such as Si and Ge in this study, for deep-level (more-than half-gap and even full-gap) 2-energy-level impurities which can trap only under transient but not steady-state.

2. Theory and Results

The formulas used in the HFCV and LFCV calculations are those used in the previous reports[2−4] for the 2-charge-state 1-energy-level impurity centers. In this report, these earlier formulas are extended to the 3-charge-state 2-energy-level impurities following that of Ref. [1] which used the distribution or occupancy by trapped electrons or holes on the 3-charge-state 2-energy level impurities given by the 1958 Sah-Shockley formulation[5].

The MOSCVs computed in this paper are in silicon, containing three impurity species. These are the 2-charge-state 1-shallow-energy-level dopants, the Group-V donor (phosphorus) and Group-III acceptor (boron), and the five 3-charge-state 2-deep-energy level impurities. We used the following four model impurities from Group IB (Au), IIB (Zn), VIB (S or Sulfur), and VIIIA (Fe). The Group IB silver (Ag) with its nearly symmetrically placed 1-donor and 1-acceptor energy level, is modeled for the ideal perfectly symmetrical case. These impurities are selected solely and only as model representatives since their trapping energy levels were not so precisely determined experimentally[4] and predicted theoretically, although firmly physics based, only be taken as empirical because of the large central cell perturbation known as the core charge difference between the host and the foreign atoms[6].

The CV curves are computed for the four impurities (S, Fe, Zn, Au) in pure or not-doped silicon, n-doped (phosphorus donor doped) and p-doped (boron acceptor doped) silicon,
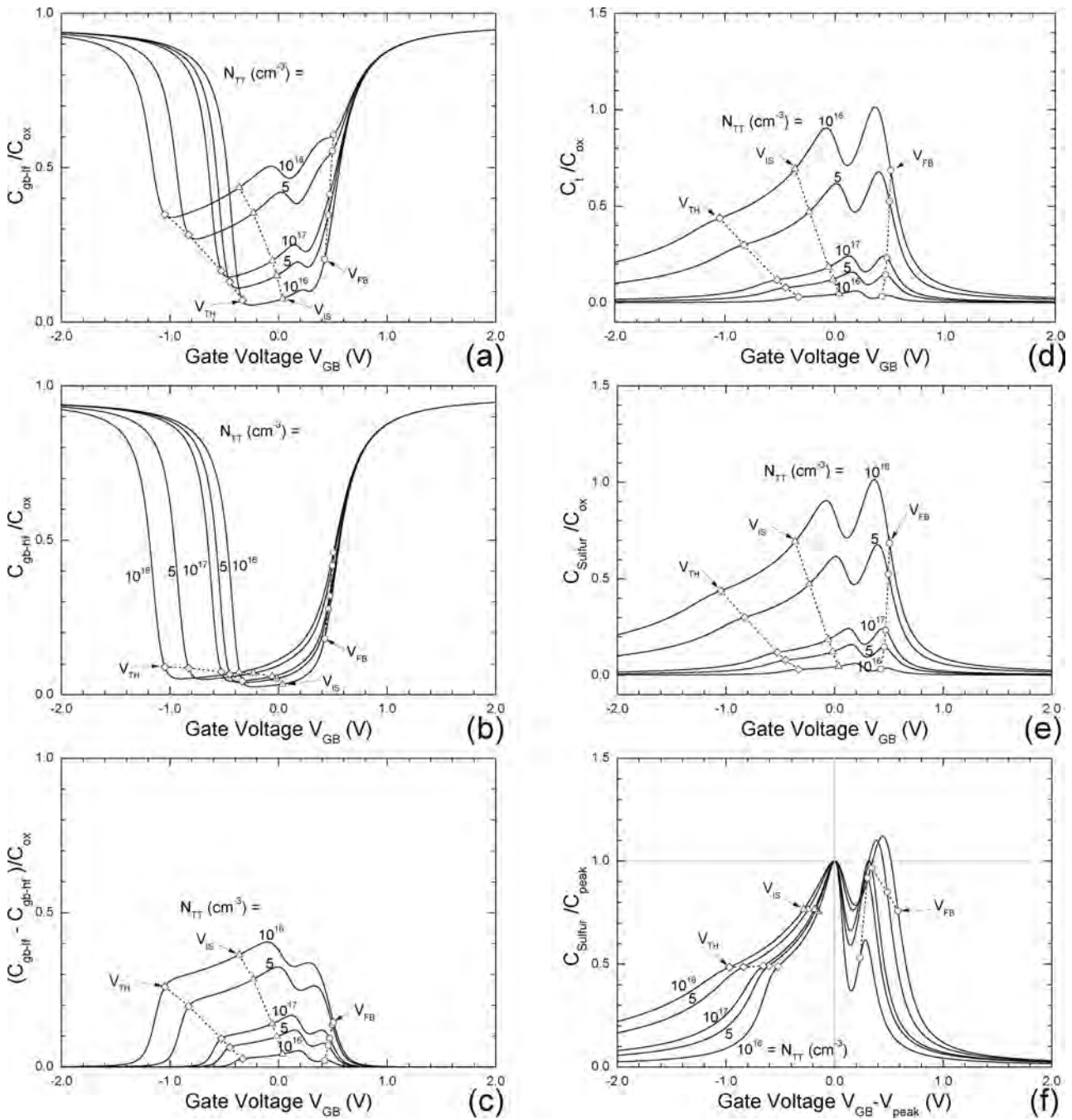
Fig. 1. Capacitance–Voltage curves of not-doped-Si MOSCs containing Sulfur, a substitutional 2-electron trap. $X_{ox} = 3.5$ nm. $T = 300$ K. $N_{DD} = P_{AA} = 0$. $N_{TT} = (1, 5, 10, 50, 100) \times 10^{16}$ S/cm^3. $E_C - E_{Sulfur-1electron} = 380$ meV. $g_{Sulfur-1electron} = 2$. $E_C - E_{Sulfur-2electron} = 180$ meV. $g_{Sulfur-2electron} = 1$. (a) C_{gb-lf}. (b) C_{gb-hf}. (c) $C_{gb-lf} - C_{gb-hf}$. (d) C_t. (e) C_{Sulfur}. (f) Normalized-Shifted C_{Sulfur}.

and exact-compensation-doped (equal phosphorus and boron concentrations to simulate the boundary of the p/n junction) with dopant concentrations fixed at 10^{18} cm^{-3} and the impurity concentration varied to cover the range of 10^{16}cm^{-3} to the impurities' maximum solid-solubility limit in Si $\sim 10^{18}$ cm^{-3}. These four impurities and four dopant combinations, give sixteen figures. Figure 17 is the complete symmetry case with the amphoteric silver as the model. Figure 18 gives a classical example that was computed and plotted, both by hands, 50 years ago.

The six sub-figures in each of the seventeen newly computed figures are (a) LFCV, (b) HFCV, (c) (LF–HF) CV,

(d) C_{trap}V including the dopants, (e) $C_{impurity}$V excluding the dopants, and (f) Normalized impurity-trap capacitance versus shifted gate-voltage, ($C_{impurity}/C_{peak}$) versus ($V_{GB} - V_{GBpk}$). The data used are given in the captions of each of the eighteen figures.

For the first three CV figures, Figs. 1 to 3, we selected the double-donor or two-electron trap, the group-VIB Sulfur, which has six outer shell or valence electrons, therefore, two of the six valence electrons can be released to the conduction band of silicon with the remaining four to satisfy the four tetrahedrally located covalent bonds of the diamond lattice of silicon. We also leverage the similarity of the sulfur core charge
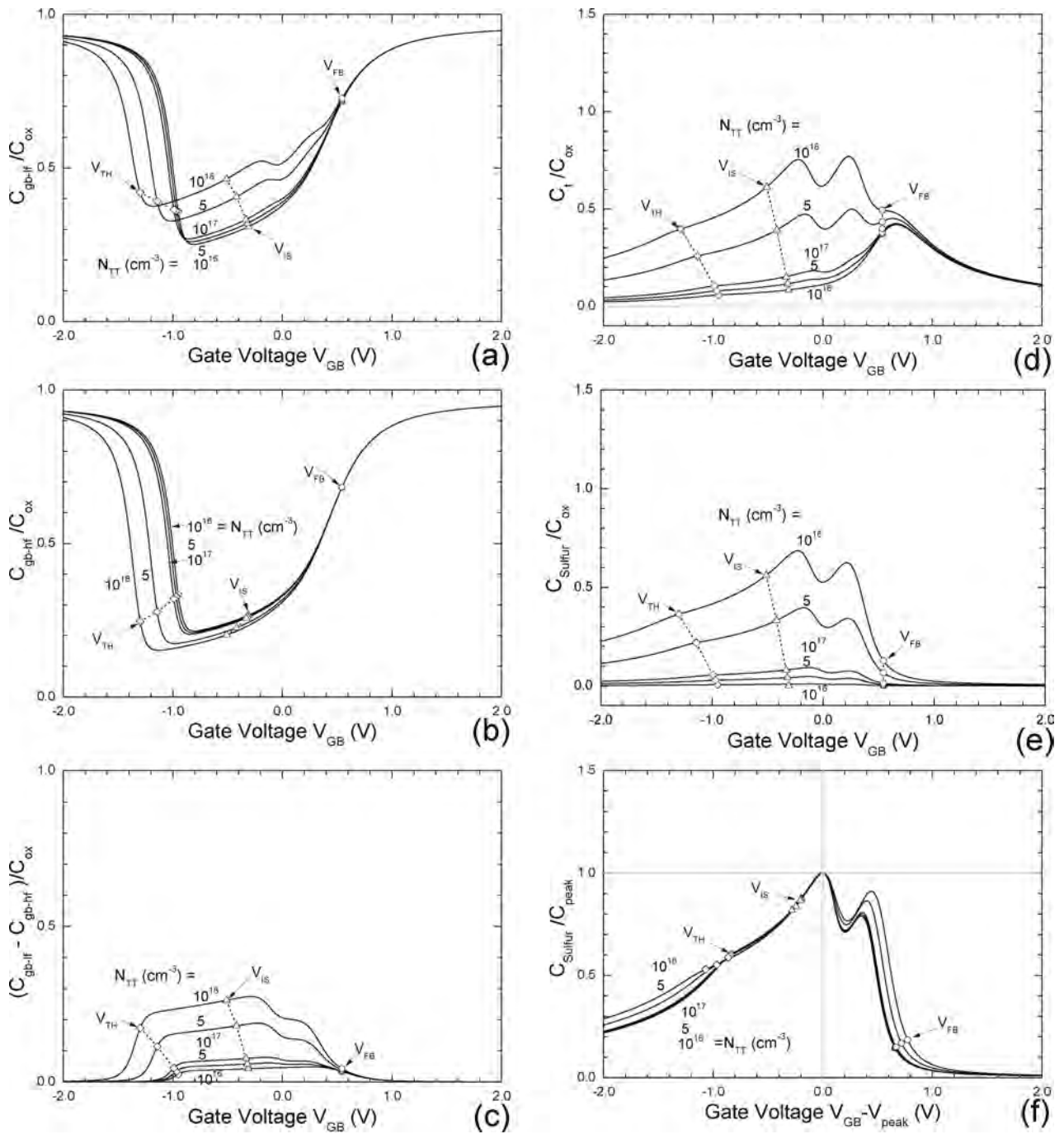
Fig. 2. Capacitance–Voltage curves of n-doped Si MOSCs containing Sulfur, a substitutional 2-electron trap. $X_{\text{ox}} = 3.5$ nm. $T = 300$ K. $P_{\text{AA}} = 0$. $N_{\text{DD}} = 10^{18}$ As/cm^3. $E_{\text{C}} - E_{\text{D}} = 49$ meV. $g_{\text{D}} = 2$. $N_{\text{TT}} = (1, 5, 10, 50, 100) \times 10^{16}$ S/cm^3. $E_{\text{C}} - E_{\text{Sulfur-1electron}} = 380$ meV. $g_{\text{Sulfur-1electron}} = 2$. $E_{\text{C}} - E_{\text{Sulfur-2electron}} = 180$ meV. $g_{\text{Sulfur-2electron}} = 1$. (a) $C_{\text{gb-lf}}$. (b) $C_{\text{gb-hf}}$. (c) $C_{\text{gb-lf}} - C_{\text{gb-hf}}$. (d) C_{t}. (e) C_{Sulfur}. (f) Normalized-Shifted C_{Sulfur}.

to that of the silicon core, namely Sulfur is isocoric to Silicon, as coined by Pantelides, Ning and Sah[6], therefore not such a large perturbation. See the Slater Table given in Ref. [7] for the core charge distribution and hence the core charge difference, via the outer-most maximum of the radial charge density variation.

For the second three figures, Figs. 4, 5 and 6, we select a second double-donor or two-electron trap, the Group VIIIA iron, Fe, with two outer shell or valence electrons, to model the huge core perturbation from the large difference between the

Fe ($Z = 26$) and Si ($Z = 14$) core-charge distributions. The difference is so huge that the one-electron donor ground state is perturbed down so deep from the conduction band edge that it is below the Si midgap, $E_{\text{C}} - E_{\text{Fe2+}} = 800$ meV, while the two-electron Fe donor state is near the midgap, $E_{\text{C}} - E_{\text{Fe1+}} = 550$ meV. If the Fe^{2+} 1-electron ground state were deeper, down to the Si valence band edge, at $k = (0.8, 0, 0)$, away from the $k = (0, 0, 0)$ valence band edge, on account of the indirect energy band of Si, then, this Fe-model donor ground state would be occupied by a hole tunneled from the valence
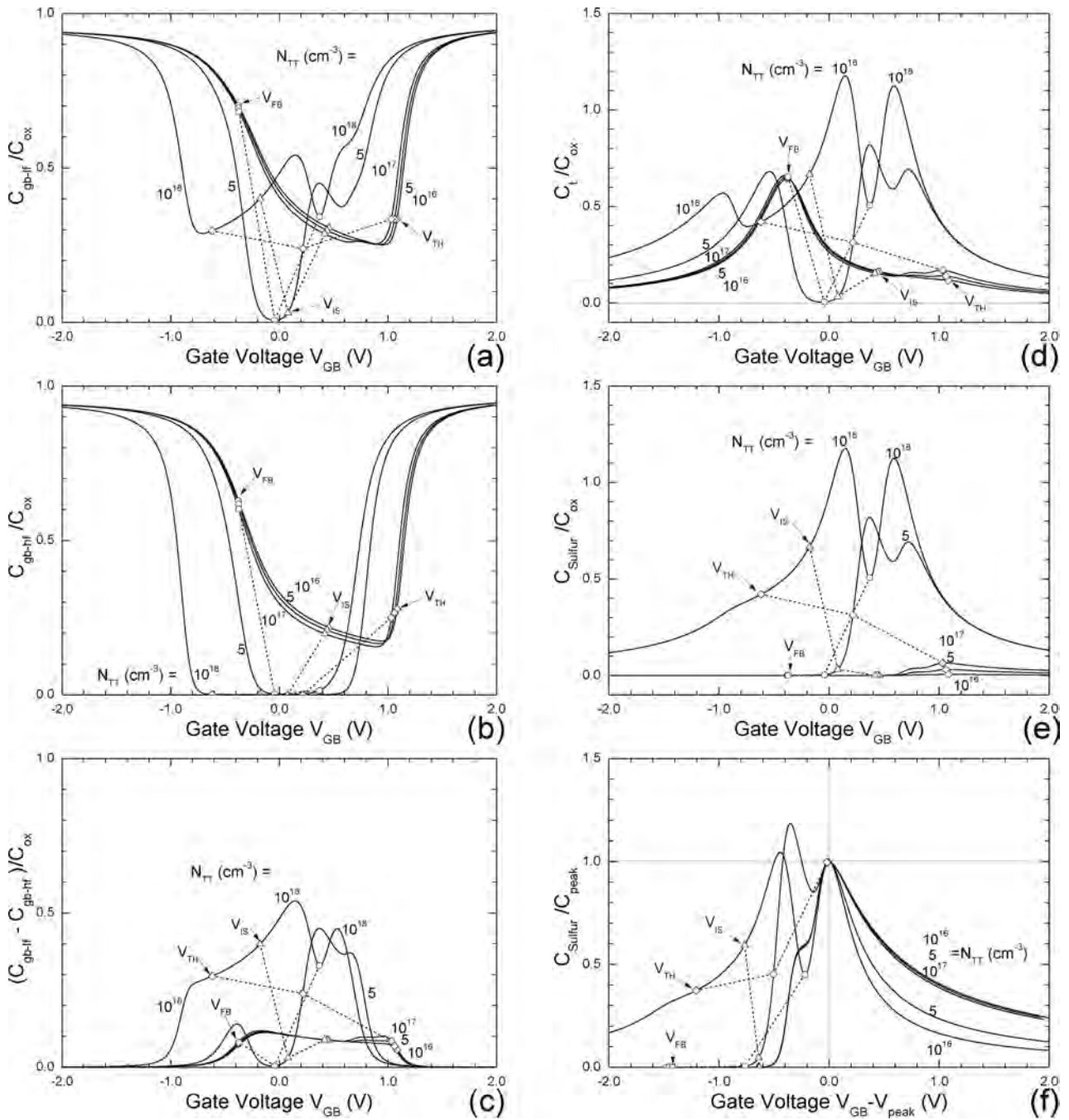
Fig. 3. Capacitance–Voltage curves of p-doped Si MOSCs containing Sulfur, a substitutional 2-electron trap. $X_{ox} = 3.5$ nm. $T = 300$ K. $N_{DD} = 0$. $P_{AA} = 10^{18}$ B/cm^3. $E_A - E_V = 45$ meV. $g_A = 4$. $N_{TT} = (1, 5, 10, 50, 100) \times 10^{16}$ S/cm^3. $E_C - E_{Sulfur-1electron} = 380$ meV. $g_{Sulfur-1electron} = 2$. $E_C - E_{Sulfur-2electron} = 180$ meV. $g_{Sulfur-2electron} = 1$. (a) C_{gb-lf}. (b) C_{gb-hf}. (c) $C_{gb-lf} - C_{gb-hf}$. (d) C_t. (e) C_{Sulfur}. (f) Normalized-Shifted C_{Sulfur}.

band. Then, the occupation of the two donor energy levels to give the three donor charge states cannot persist and are always not occupied, or Fe donor is always in the doubly positively charged state, and the other two charge states, singly charged and neutral, cannot exist under equilibrium or nonequilibrium d. c. steady-state, only under transient (faster than the tunneling rate, phonon assisted to supply the k change). The lower Fe donor energy level, $E_C - E_{Fe2+} = 800$ meV, reported in the 1960's[4], was not so deep down to a level at or below the valence band edge of silicon. But this example offers an interesting possibility of hidden charge states that are only observ-

able under fast enough transient before the valence band hole can tunnel to the hole trap.

For the third group of three CV figures, Figs. 7, 8, and 9, we selected the Group-IIB Zinc-like double acceptors. Although zinc is not isocoric with silicon (The IIA Mg or Magnesium, $Z = 12$, is but not reported.), and Zn has much more core charge ($Z = 30$) spreading slight further (0.32A) than that of silicon ($Z = 14$ and 0.20A)[7], the core charge perturbation from the substitution zinc is still not sufficiently large to deepen the first acceptor energy level to far above the Si midgap, like the just-described model Fe. So, the two Zn acceptor levels are
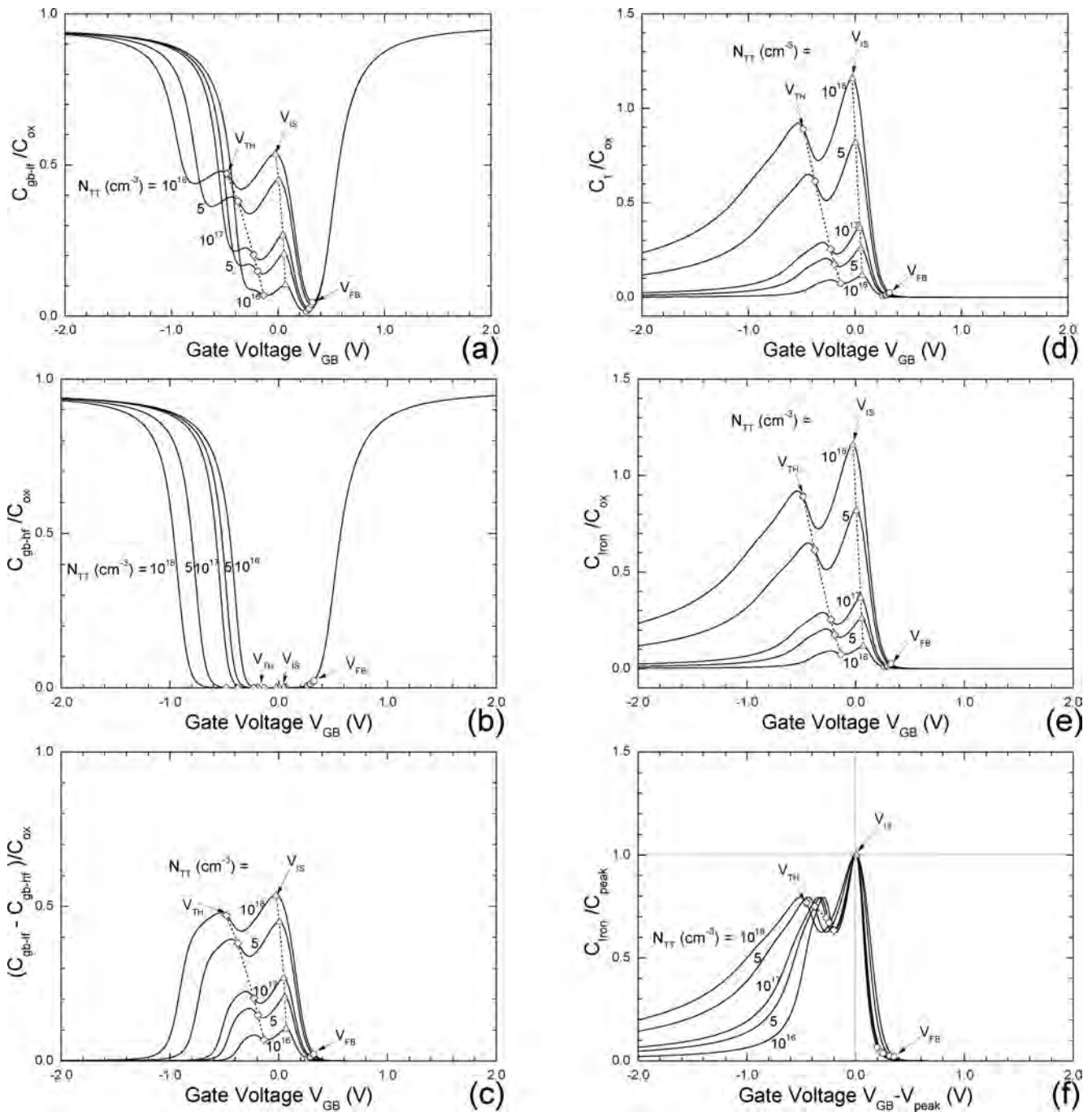
Fig. 4. Capacitance–Voltage curves of not-doped-Si MOSCs containing Iron, a substitutional 2-electron trap. X_{ox} = 3.5 nm. T = 300 K. N_{DD} = P_{AA} = 0. N_{TT} = (1, 5, 10, 50, 100) × 10^{16} Fe/cm^3. $E_C - E_{Iron-1electron}$ = 800 meV. $g_{Iron-1electron}$ = 2. $E_C - E_{Iron-2electron}$ = 550 meV. $g_{Iron-2electron}$ = 1. (a) C_{gb-lf}. (b) C_{gb-hf}. (c) $C_{gb-lf} - C_{gb-hf}$. (d) C_t. (e) C_{Iron}. (f) Normalized-Shifted C_{Iron}.

only slightly deeper than the two Sulfur donor levels. And these three CV figures for Zn in Figs. 7–9, are mirror images of the same CV curves for S in Figs. 1–3.

The three CV figures (Figs 10, 11, and 12) in the next group are for the Group-IB Gold (Au) which has one valence electron and which can trap an electron or a hole, to be the single negative or acceptor and single positive or donor charge state. This dual charge state property of either in the acceptor or the donor charge state is known in semiconductor physics as amphoteric. The origin of the presence of bound state for two complementary particles, electron and hole, can be understood from the large core charge difference between the Gold core (Z = 79) and the Silicon core (Z = 14), that enables the trapping or binding of either a conduction-band electron at $E_C - E_{Au-1electron}$ = 540 meV or a valence-band hole at $E_{Au-1hole} - E_V$ = 350 meV, to the electrically neutral gold perturbation potential.

Finally, the fifth group consists of four CV figures, instead of three, (Figs. 13, 14, 15 and 16) which are for the four model impurities just described (S, Fe, Zn and Au) in exactly compensated silicon at the equal dopant acceptor and donor concentration, equaling the maximum solubility of the impurity in silicon, with the impurity concentration as the constant para-
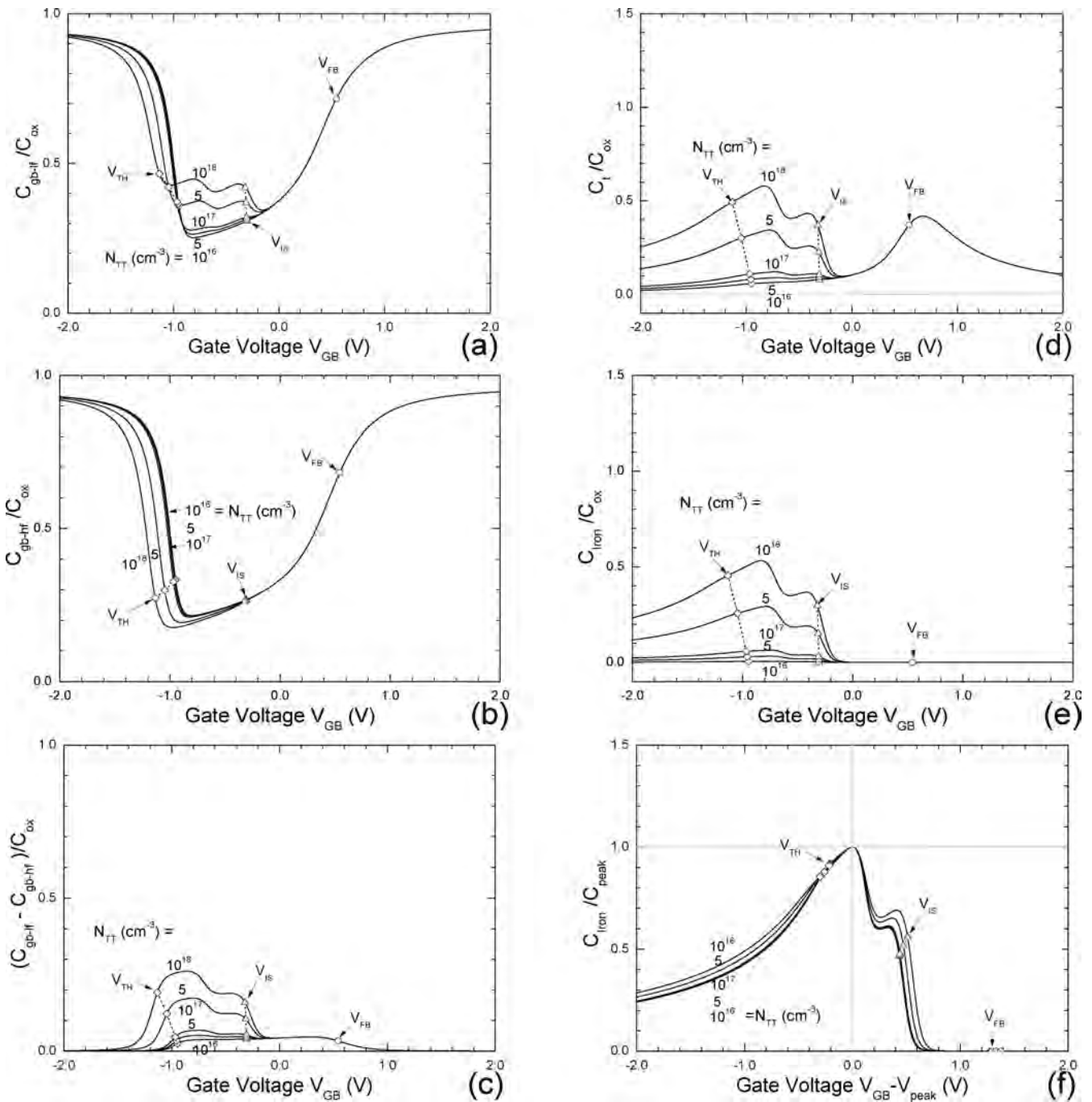
Fig. 5. Capacitance–Voltage curves of n-doped Si MOSCs containing Iron, a substitutional 2-electron trap. $X_{\mathrm{ox}} = 3.5$ nm. $T = 300$ K. $P_{\mathrm{AA}} = 0$. $N_{\mathrm{DD}} = 10^{18}$ As/cm^3. $E_{\mathrm{C}} - E_{\mathrm{D}} = 49$ meV. $g_{\mathrm{D}} = 2$. $N_{\mathrm{TT}} = (1, 5, 10, 50, 100) \times 10^{16}$ Fe/cm^3. $E_{\mathrm{C}} - E_{\mathrm{Iron\text{-}1electron}} = 800$ meV. $g_{\mathrm{Iron\text{-}1electron}} = 2$. $E_{\mathrm{C}} - E_{\mathrm{Iron\text{-}2electron}} = 550$ meV. $g_{\mathrm{Iron\text{-}2electron}} = 1$. (a) $C_{\mathrm{gb\text{-}lf}}$. (b) $C_{\mathrm{gb\text{-}hf}}$. (c) $C_{\mathrm{gb\text{-}lf}} - C_{\mathrm{gb\text{-}hf}}$. (d) C_{t}. (e) C_{Iron}. (f) Normalized-Shifted C_{Iron}.

meter increasing from a low value of 10^{15} cm^{-3} to the maximum solubility (4×10^{16} S/cm^3, 3×10^{16} Fe/cm^3, 6×10^{16} Zn/cm^3, and 12×10^{16} Au/cm^3). These are designed as model representations for the practical situation at the 'metallurgical' boundary of the p/n junction where the net dopant acceptor and donor concentrations are equal and exactly cancel each other in charge. However, they also could be used by leverage this condition for enhanced sensitivity from large trapping capacitance signals.

Figure 17 is designed to determine if there are special features in the CV curves in the case of a completely symmetri-

cal case of identical electron and hole bands and also identical electron and hole traps. The Group-IB Silver (Ag) approaches this model since it is amphoteric, like gold with one valence electron and the Silver core ($Z = 47$) charge difference from the Silicon core ($Z = 14$) charge is not so large as that of Gold ($Z = 79$) just described, so that the electron and hole binding energies are more symmetrically located with respect to the silicon midgap, $E_{\mathrm{C}} - E_{\mathrm{Ag\text{-}1electron}} = 220$ meV (540 for Au) and $E_{\mathrm{Ag\text{-}1hole}} - E_{\mathrm{V}} = 320$ meV (350 meV for Au). Silver is also of technical importance as the lifetime killer to reduce the recovery time during switching in high power Silicon Controlled
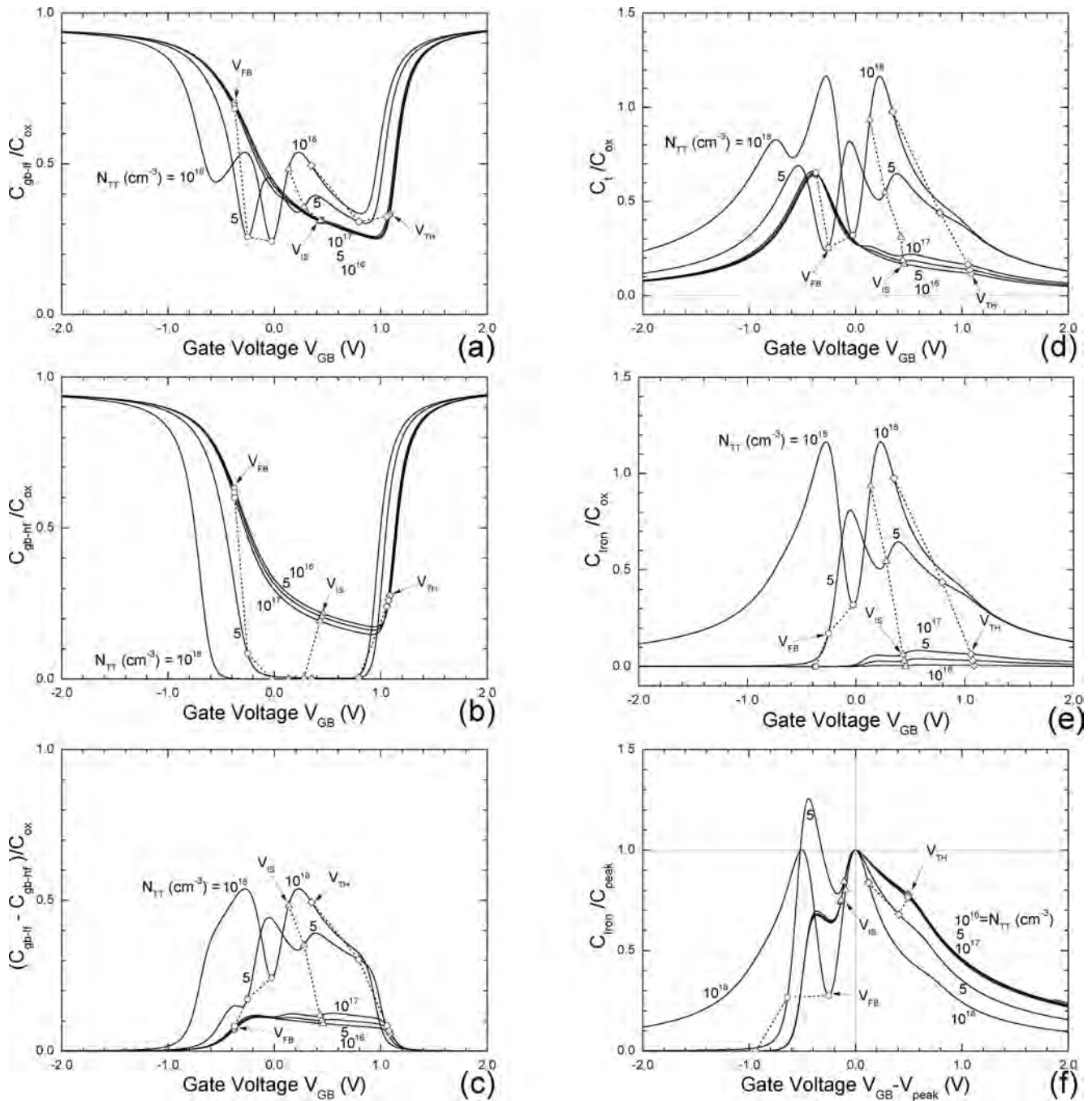
Fig. 6. Capacitance–Voltage curves of p-doped Si MOSCs containing Iron, a substitutional 2-electron trap. $X_{ox} = 3.5$ nm. $T = 300$ K. $N_{DD} = 0$. $P_{AA} = 10^{18}$ B/cm^3. $E_A - E_V = 45$ meV. $g_A = 4$. $N_{TT} = (1, 5, 10, 50, 100) \times 10^{16}$ Fe/cm^3. $E_C - E_{Iron-1electron} = 800$ meV. $g_{Iron-1electron} = 2$. $E_C - E_{Iron-2electron} = 550$ meV. $g_{Iron-2electron} = 1$. (a) C_{gb-lf}. (b) C_{gb-hf}. (c) $C_{gb-lf} - C_{gb-hf}$. (d) C_t. (e) C_{Iron}. (f) Normalized-Shifted C_{Iron}.

Rectifier[7] while not significantly increasing the leakage current during the off state. In Fig. 17, we made two trapping levels perfectly symmetrical in computing the CV curves, with the parameter values given in its figure caption. These CV curves show the complete symmetry with respect to flat-band which is slightly off from $V_{GB} = 0$ due to the inadvertent inclusion or not removing the work function difference between the aluminum metal gate and silicon body.

As a historical epilogue, Fig. 18 is a copy of the LFCV of the silicon MOSC containing gold, which was computed using slide rule and plotted by hand 50 years ago[1]. These old CV curves are nearly identical to those shown in Fig. 10(a).

3. Summary

In this study, we have demonstrated the effects on the CV curves from electron and hole trapping at impurities with two energy levels and three-charge-states in silicon MOS capacitors, which are not-doped, p-doped, n-doped and completely-compensating-doped that simulates the p/n junction boundary. Five two-energy-level three-charge-state impurities are selected as models to illustrate the CV variations. These are the double donor impurity two-electron trap, such as Sulfur, the double donor impurity two-electron deep-level trap such as Iron, the double acceptor impurity two-hole trap such as
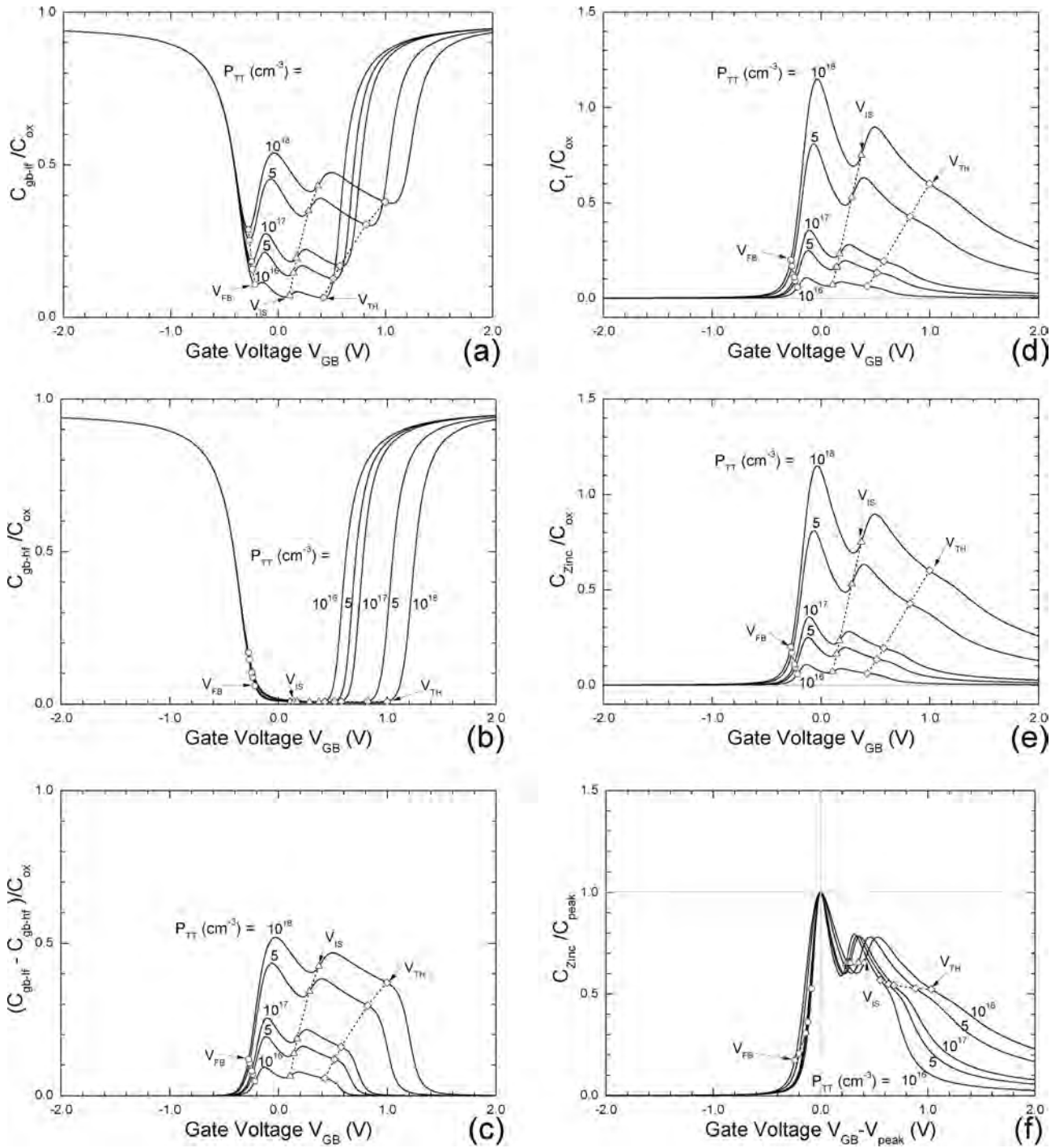
Fig. 7. Capacitance–Voltage curves of not-doped-Si MOSCs containing Zinc, a substitutional 2-hole trap. $X_{ox} = 3.5$ nm. $T = 300$ K. $N_{DD} = P_{AA} = 0$. $P_{TT} = (1, 5, 10, 50, 100) \times 10^{16}$ Zn/cm^3. $E_{Zinc\text{-}1hole} - E_V = 660$ meV. $g_{Zinc\text{-}1hole} = 4$. $E_{Zinc\text{-}2hole} - E_V = 310$ meV. $g_{Zinc\text{-}2hole} = 2$. (a) $C_{gb\text{-}lf}$. (b) $C_{gb\text{-}hf}$. (c) $C_{gb\text{-}lf} - C_{gb\text{-}hf}$. (d) C_t. (e) C_{Zinc}. (f) Normalized-Shifted C_{Zinc}.

Zinc, the amphoteric impurity deep-level 1-electron and 1-hole trap such as gold, and the amphoteric impurity mid-deep-level 1-electron and 1-hole trap such as silver. We also presented the CV curves of a MOSC which has the idealized complete-symmetry of band electrons and holes and also trapped electron and hole at the idealized 1-electron and 1-hole amphoteric impurity. The results of these exercises, hopefully, will provide the guide for more accurate or new experimental characterization of the fundamental parameters (energy levels, charge states, and eventually excited states and kinetic rate coeffi-

cients) of these impurity traps, and will also provide a guide for potential applications of the trapping capacitance in MOS devices with high sensitivity in the sub-millimeter and far infrared ranges, in addition to the p/n/p/n Silicon Controlled Rectifiers with lower power dissipation[7] and the terrestrial solar cells with improved efficiency[8].

References

[1] Sah Chih-Tang, "Theory of the Metal Oxide Semiconductor
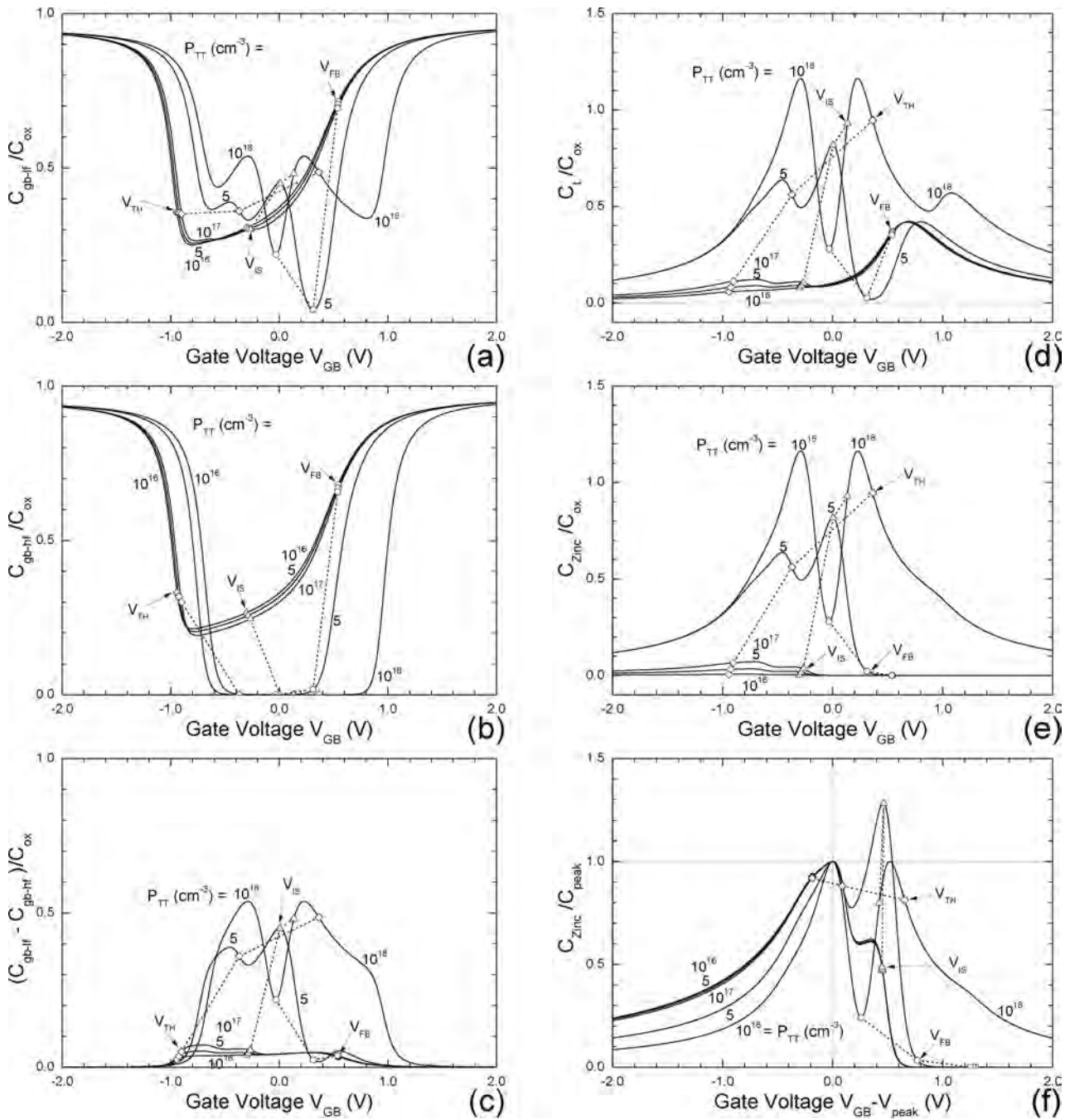
Fig. 8. Capacitance–Voltage curves of n-doped Si MOSCs containing Zinc, a substitutional 2-hole trap. $X_{ox} = 3.5$ nm. $T = 300$ K. $P_{AA} = 0$. $N_{DD} = 10^{18}$ As/cm^3. $E_C - E_D = 49$ meV. $g_D = 2$. $P_{TT} = (1, 5, 10, 50, 100) \times 10^{16}$ Zn/cm^3. $E_{Zinc\text{-}1hole} - E_V = 660$ meV. $g_{Zinc\text{-}1hole} = 4$. $E_{Zinc\text{-}2hole} - E_V = 310$ meV. $g_{Zinc\text{-}2hole} = 2$. (a) $C_{gb\text{-}lf}$. (b) $C_{gb\text{-}hf}$. (c) $C_{gb\text{-}lf} - C_{gb\text{-}hf}$. (d) C_t. (e) C_{Zinc}. (f) Normalized-Shifted C_{Zinc}.

Capacitor," Technical Report No.1, $\sim$155 pages and $\sim$55 figures, Solid-State Electronics Laboratory, University of Illinois at Urbana-Champaign (UIUC), December 14, 1964; Fourth Printing, February 1974. 300 total copies printed and sent to requesters. Scanned digital copy at low but legible resolution now available to qualified researchers by email request to the author.

[2] Jie Binbin and Sah Chihtang, "MOS Capacitance–Voltage Characteristics from Electron-Trapping at Dopant Donor Impurity," Journal of Semiconductors, 32(4), 041001-1–9, April 2011.

[3] Jie Binbin and Sah Chihtang, "MOS Capacitance–Voltage Characteristics: II. Sensitivity of Electronic Trapping at Dopant Impurity from Parameter Variations," Journal of Semiconductors, 32(12), 121001-1–11, December 2011.

[4] Jie Binbin and Sah Chihtang, "MOS Capacitance–Voltage Characteristics: III. Trapping Capacitance from 2-Charge-State Impurities," Journal of Semiconductors, 32(12), 121002-1–16, December 2011.

[5] Sah Chih-Tang and Shockley William, "Electron–Hole Recombination Statistics in Semiconductors through Flaws with Many Charge Conditions," Physical Review, 109(4), 1103–1115, February 15, 1958.

[6] Pantelides Sokrate T and Sah Chih-Tang, "Theory of Localized States in Semiconductors. I. New Results Using an Old Method," Physical Review B, 10(2), 621–637, July 15, 1974. Pantelides Sokrate T and Sah Chih-Tang, "Theory of Localized States in Semiconductors. II. The Pseudo Impurity Theory Application to
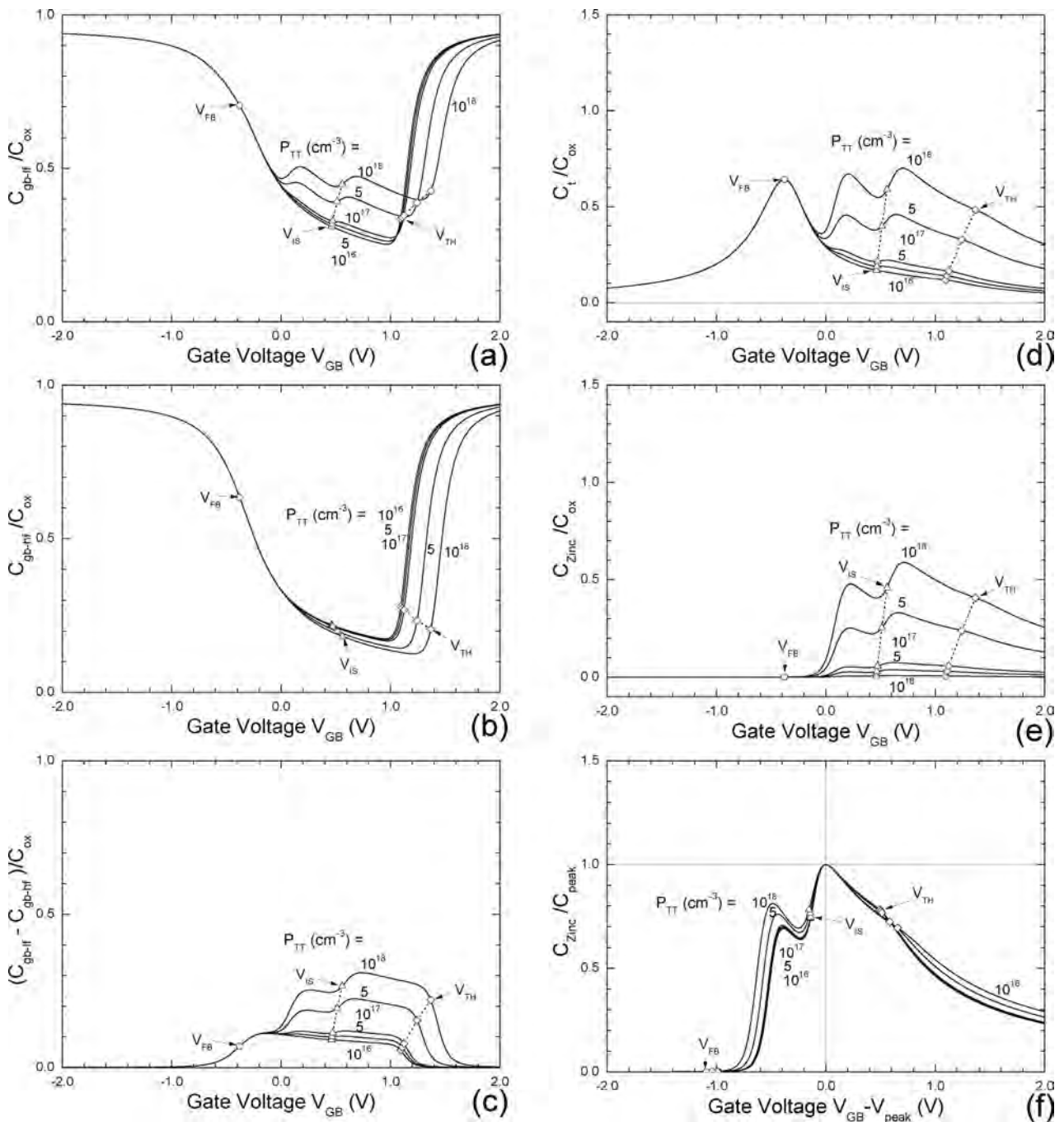
Fig. 9. Capacitance–Voltage curves of p-doped Si MOSCs containing Zinc, a substitutional 2-hole trap. $X_{ox} = 3.5$ nm. $T = 300$ K. $N_{DD} = 0$. $P_{AA} = 10^{18}$ B/cm^3. $E_A - E_V = 45$ meV. $g_A = 4$. $P_{TT} = (1, 5, 10, 50, 100) \times 10^{16}$ Zn/cm^3. $E_{Zinc-1hole} - E_V = 660$ meV. $g_{Zinc-1hole} = 4$. $E_{Zinc-2hole} - E_V = 310$ meV. $g_{Zinc-2hole} = 2$. (a) C_{gb-lf}. (b) C_{gb-hf}. (c) $C_{gb-lf} - C_{gb-hf}$. (d) C_t. (e) C_{Zinc}. (f) Normalized-Shifted C_{Zinc}.

Shallow and Deep Donors in Silicon," Physical Review B, 10(2), 638–658, July 15, 1974. Ning Tak H. and Sah Chih-Tang, "Multivalley Effective-Mass Approximation for Donor States in Silicon. I. Shallow-Level Group-V Impurities," Physical Review B, 4(10), 3468–3481, November 15, 1971. Ning Tak H. and Sah Chih-Tang, "Multivalley Effective-Mass Approximation for Donor States in Silicon. II. Deep-Level Group-VI Double-Donor Impurities," Physical Review B, 4(10), 3482–3488, November 15, 1971. Ning Tak H. and Sah Chih-Tang, "Photoionization Cross Section of a Two-electron Donor Center in Silicon," Phys-

ical Review B, 14(6), 2528–2533, September 15, 1976.
[7] Sah Chih-Tang, Fundamentals of Solid State Electronics, 1001 page, 1991. World Scientific Publishing Company, Singapore. See the Slater Tables on pages 90 and 91. See the silicon p/n/p/n diode and triode, known as SCR, described in Sections 780 to 783 on pages 955 to 979.
[8] Sah Chih-Tang, Chan Philip Ching Ho, Wang Chi-Kuo, Sah Robert L-Y, Yamakawa K. Alan, and Lutwack Ralph, "Effect of Zinc Impurity on Silicon Solar-Cell Efficiency," IEEE Transactions on Electron Devices, 28(3), 304–313, March 1981.
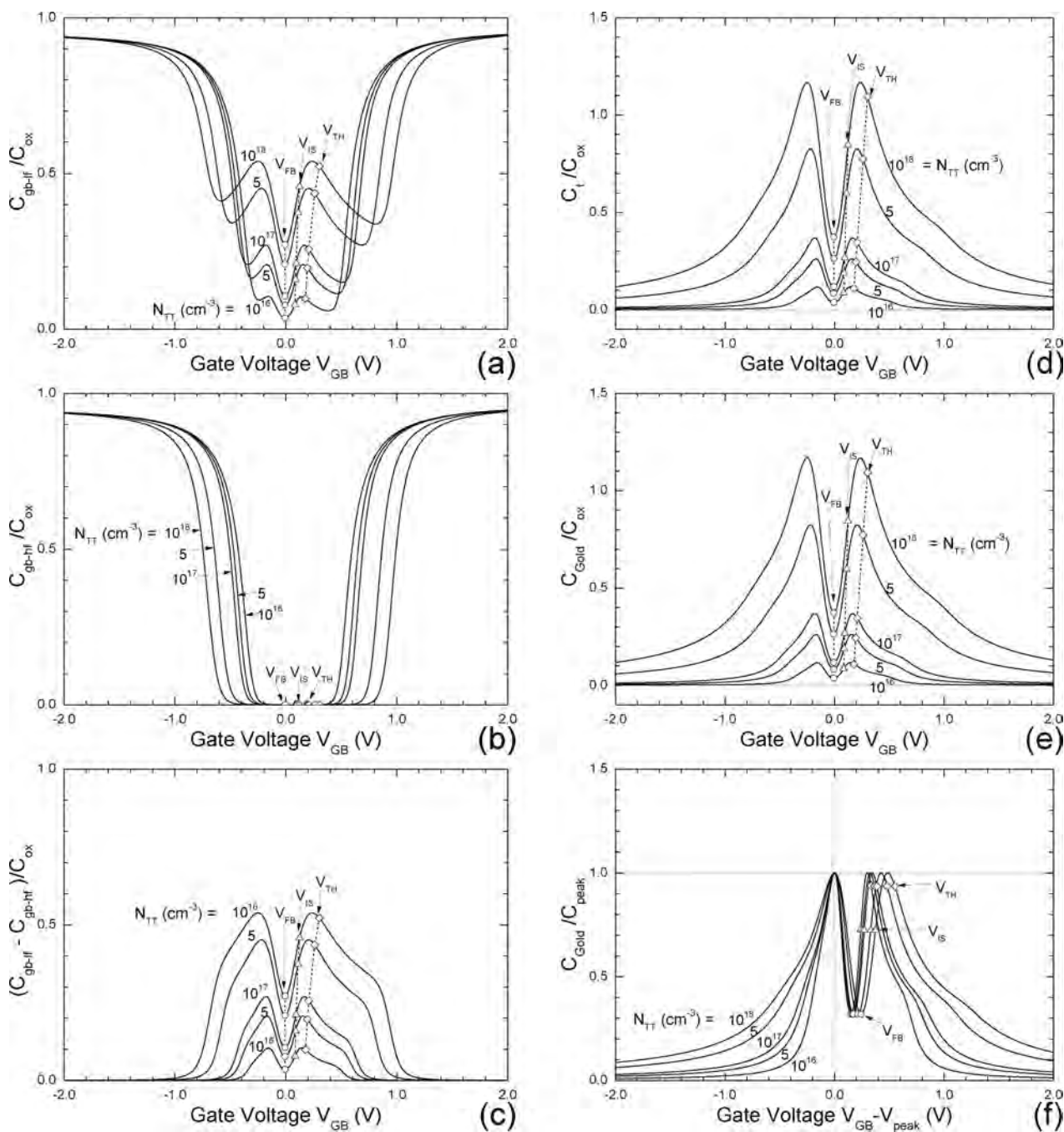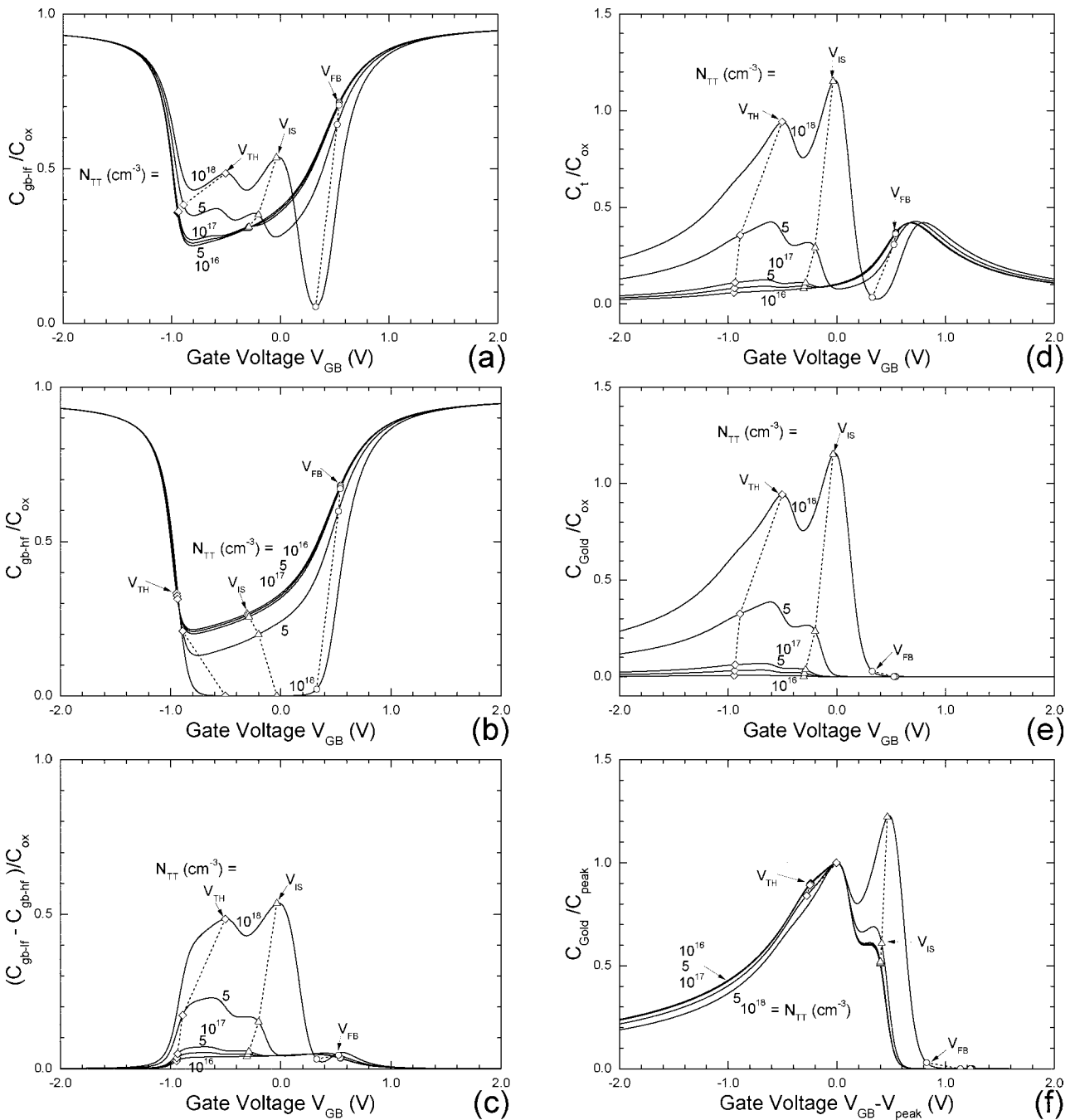
Fig. 10. Capacitance–Voltage curves of not-doped-Si MOSCs containing Gold, a substitutional amphoteric 1-electron and 1-hole trap. $X_{ox} =$ 3.5 nm. $T = 300$ K. $N_{DD} = P_{AA} = 0$. $N_{TT} = (1, 5, 10, 50, 100) \times 10^{16}$ Au/cm^3. $E_C − E_{\text{Gold-1hole}} = 540$ meV. $g_{\text{Gold-1hole}} = 3$. $E_{\text{Gold-1electron}} − E_V = 350$ meV. $g_{\text{Gold-1electron}} = 1$. (a) $C_{\text{gb-lf}}$. (b) $C_{\text{gb-hf}}$. (c) $C_{\text{gb-lf}} − C_{\text{gb-hf}}$. (d) C_t. (e) C_{Gold}. (f) Normalized-Shifted C_{Gold}.
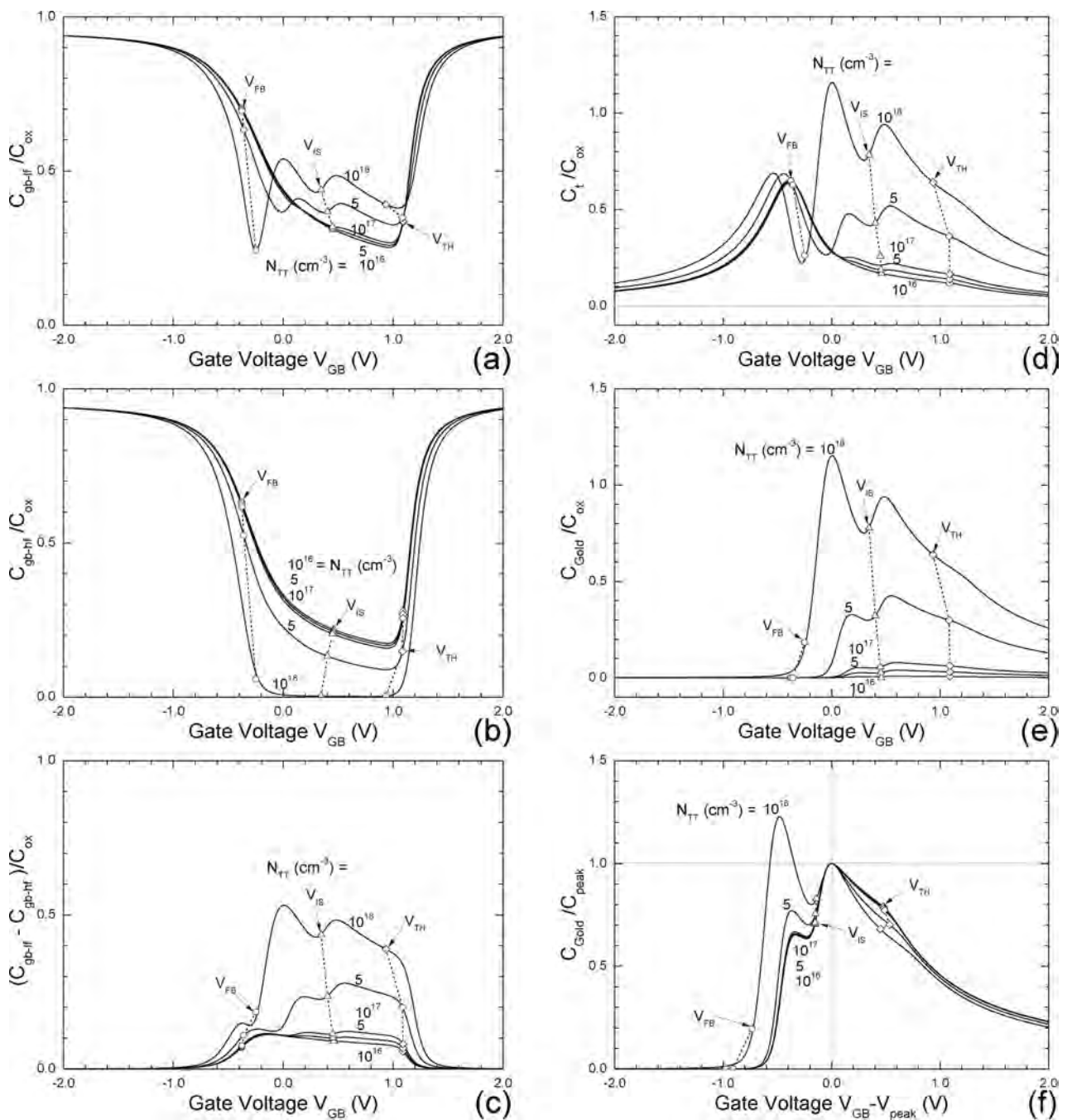
Fig. 11. Capacitance–Voltage curves of n-doped Si MOSCs containing Gold, a substitutional amphoteric 1-electron and 1-hole trap. $X_{ox} = 3.5$ nm. $T = 300$ K. $P_{AA} = 0$. $N_{DD} = 10^{18}$ As/cm^3. $E_C - E_D = 49$ meV. $g_D = 2$. $N_{TT} = (1, 5, 10, 50, 100) \times 10^{16}$ Au/cm^3. $E_C - E_{Gold\text{-}1hole}$ = 540 meV. $g_{Gold\text{-}1hole} = 3$. $E_{Gold\text{-}1electron} - E_V = 350$ meV. $g_{Gold\text{-}1electron} = 1$. (a) $C_{gb\text{-}lf}$. (b) $C_{gb\text{-}hf}$. (c) $C_{gb\text{-}lf} - C_{gb\text{-}hf}$. (d) C_t. (e) C_{Gold}. (f) Normalized-Shifted C_{Gold}.

Fig. 12. Capacitance–Voltage curves of p-doped Si MOSCs containing Gold, a substitutional amphoteric 1-electron and 1-hole trap. $X_{ox} = 3.5$ nm. $T = 300$ K. $N_{DD} = 0$. $P_{AA} = 10^{18}$ B/cm^3. $E_A - E_V = 45$ meV. $g_A = 4$. $N_{TT} = (1, 5, 10, 50, 100) \times 10^{16}$ Au/cm^3. $E_C - E_{Gold\text{-}1hole}$ $= 540$ meV. $g_{Gold\text{-}1hole} = 3$. $E_{Gold\text{-}1electron} - E_V = 350$ meV. $g_{Gold\text{-}1electron} = 1$. (a) $C_{gb\text{-}lf}$. (b) $C_{gb\text{-}hf}$. (c) $C_{gb\text{-}lf} - C_{gb\text{-}hf}$. (d) C_t. (e) C_{Gold}. (f) Normalized-Shifted C_{Gold}.
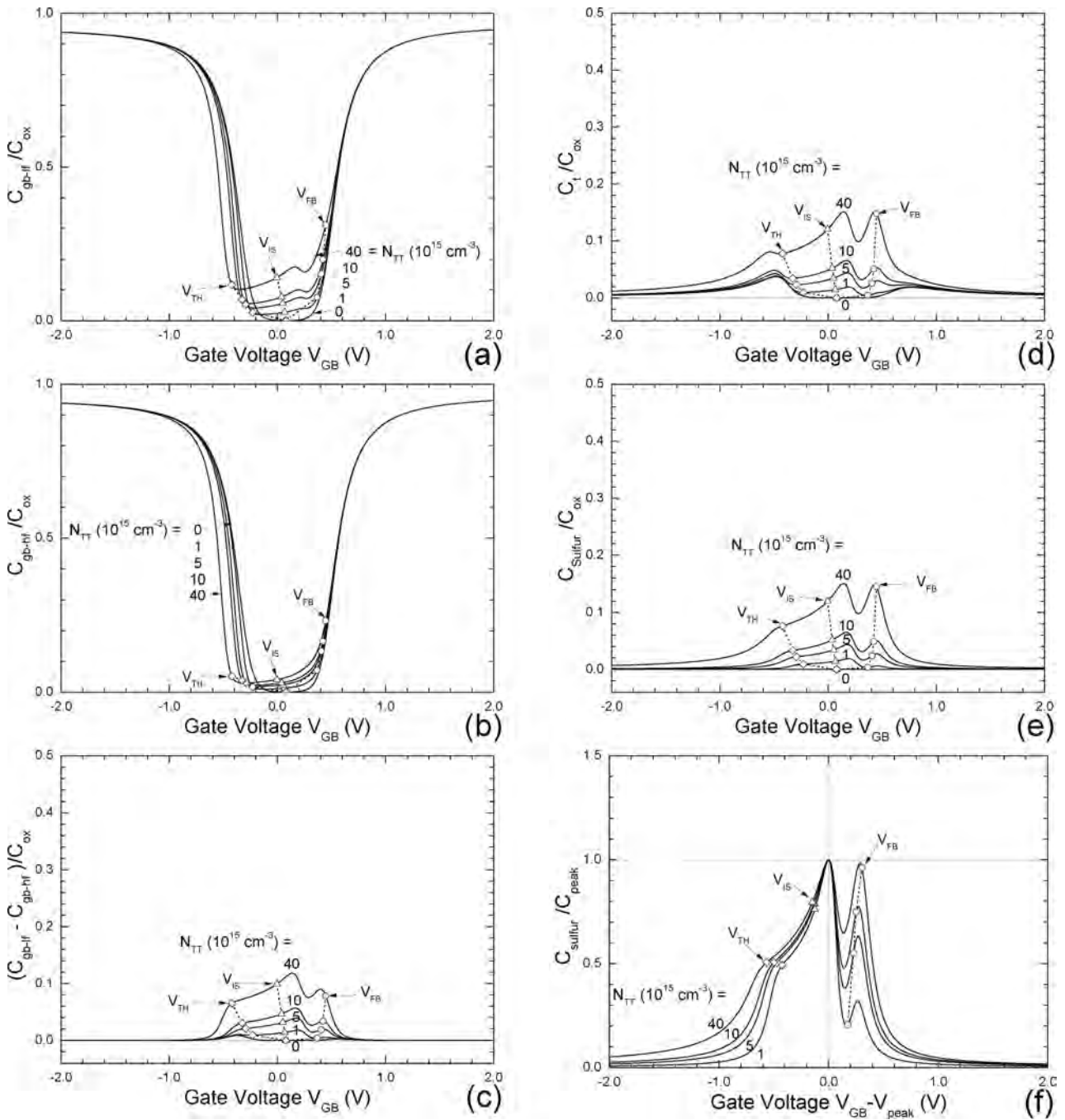
Fig. 13. $C-V$ curves of compensated Si MOSCs containing a model Sulfur, a substitutional 2-electron trap. $X_{ox} = 3.5$ nm. $T = 300$ K. $N_{DD} = P_{AA} = 40 \times 10^{15}$ cm^{-3}. $E_C - E_D = E_A - E_V = 50$ meV. $g_D = 2$. $g_A = 4$. $N_{TT} = (0, 1, 5, 10, 40) \times 10^{15}$ S/cm^3. $E_C - E_{Sulfur-1electron} = 400$ meV. $g_{Sulfur-1electron} = 2$. $E_C - E_{Sulfur-2electron} = 200$ meV. $g_{Sulfur-2electron} = 1$. (a) C_{gb-lf}. (b) C_{gb-hf}. (c) $C_{gb-lf} - C_{gb-hf}$. (d) C_t. (e) C_{Sulfur}. (f) Normalized-Shifted C_{Sulfur}.
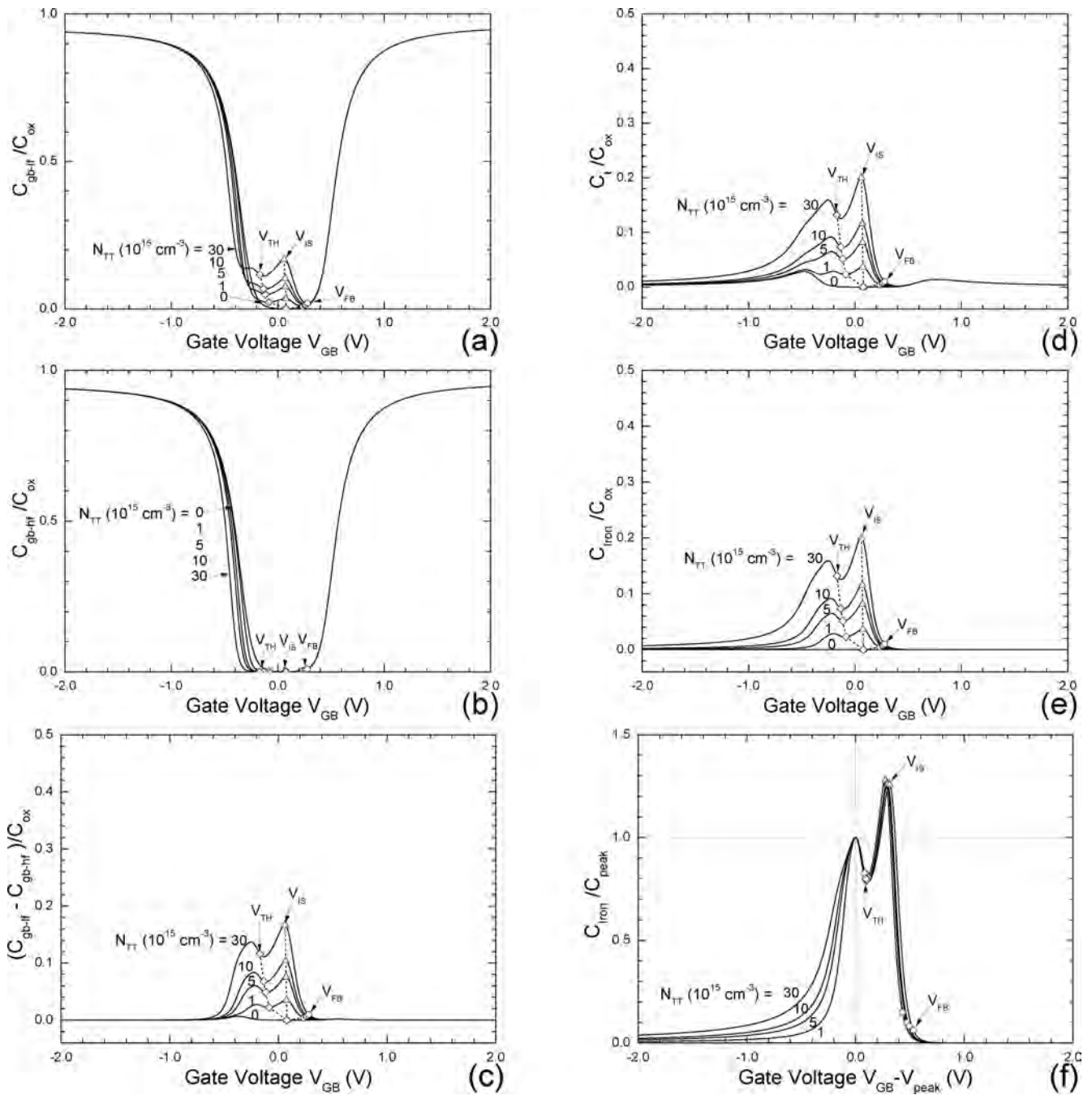
Fig. 14. C–V curves of compensated Si MOSCs containing a <u>model</u> Iron, a substitutional 2-electron trap. $X_{\mathrm{ox}} = 3.5$ nm. $T = 300$ K. $N_{\mathrm{DD}} = P_{\mathrm{AA}} = 30 \times 10^{15}$ cm^{-3}. $E_{\mathrm{C}} - E_{\mathrm{D}} = E_{\mathrm{A}} - E_{\mathrm{V}} = 50$ meV. $g_{\mathrm{D}} = 2$. $g_{\mathrm{A}} = 4$. $N_{\mathrm{TT}} = (0, 1, 5, 10, 30) \times 10^{15}$ Fe/cm^3. $E_{\mathrm{C}} - E_{\mathrm{Iron\text{-}1electron}} = 800$ meV. $g_{\mathrm{Iron\text{-}1electron}} = 2$. $E_{\mathrm{C}} - E_{\mathrm{Iron\text{-}2electron}} = 550$ meV. $g_{\mathrm{Iron\text{-}2electron}} = 1$. (a) $C_{\mathrm{gb\text{-}lf}}$. (b) $C_{\mathrm{gb\text{-}hf}}$. (c) $C_{\mathrm{gb\text{-}lf}} - C_{\mathrm{gb\text{-}hf}}$. (d) C_{t}. (e) C_{Iron}. (f) Normalized-Shifted C_{Iron}.
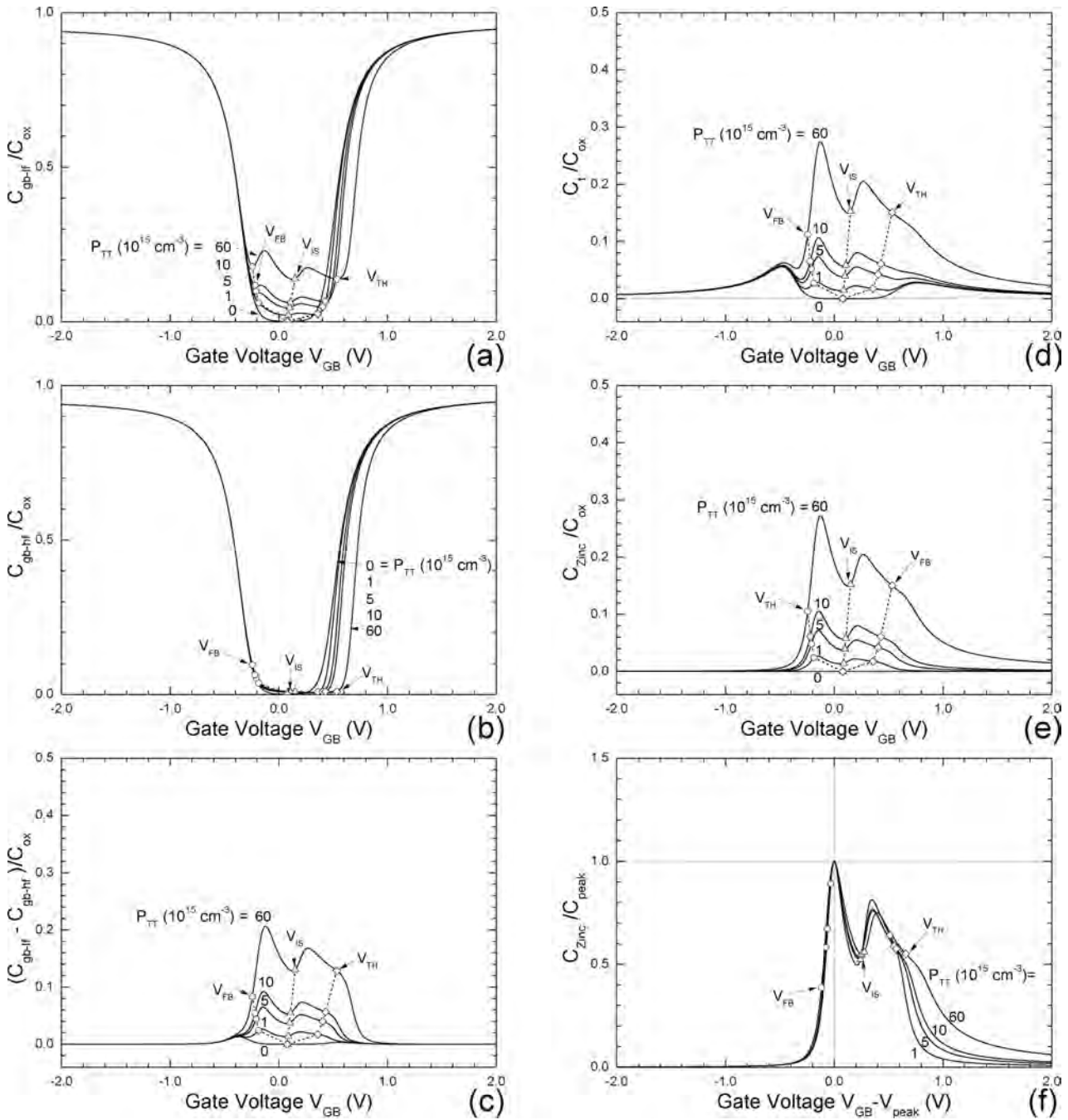
Fig. 15. C–V curves of compensated Si MOSCs containing a <u>model</u> Zinc, a substitutional 2-hole trap. $X_{ox} = 3.5$ nm. $T = 300$ K. $N_{DD} = P_{AA}$ $= 60 \times 10^{15}$ cm^{-3}. $E_C - E_D = E_A - E_V = 50$ meV. $g_D = 2$. $g_A = 4$. $P_{TT} = (0, 1, 5, 10, 60) \times 10^{15}$ Zn/cm^3. $E_{Zinc\text{-}1hole} - E_V = 600$ meV. $g_{Zinc\text{-}1hole} = 4$. $E_{Zinc\text{-}2hole} - E_V = 300$ meV. $g_{Zinc\text{-}2hole} = 2$. (a) $C_{gb\text{-}lf}$. (b) $C_{gb\text{-}hf}$. (c) $C_{gb\text{-}lf} - C_{gb\text{-}hf}$. (d) C_t. (e) C_{Zinc}. (f) Normalized-Shifted C_{Zinc}.
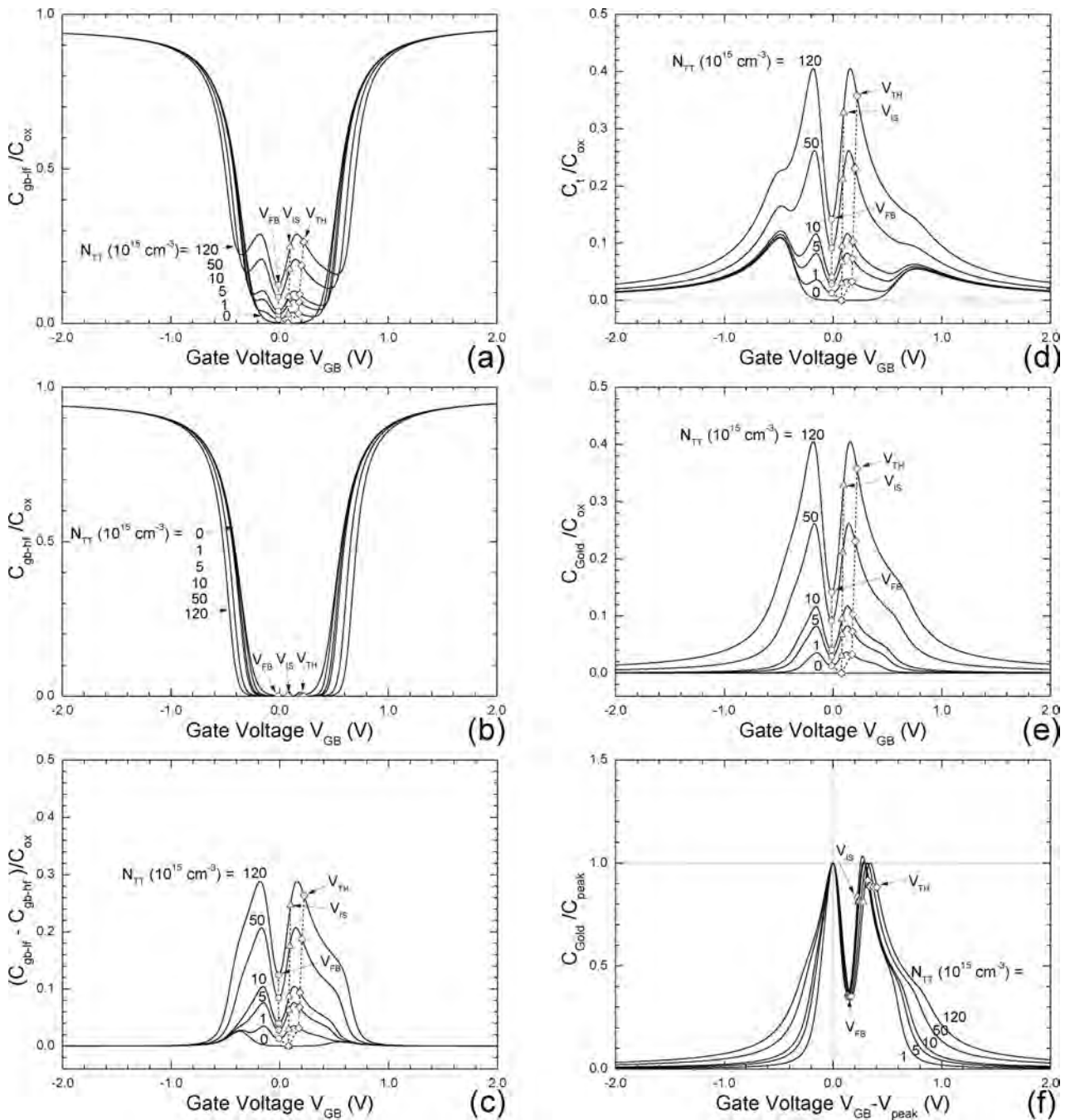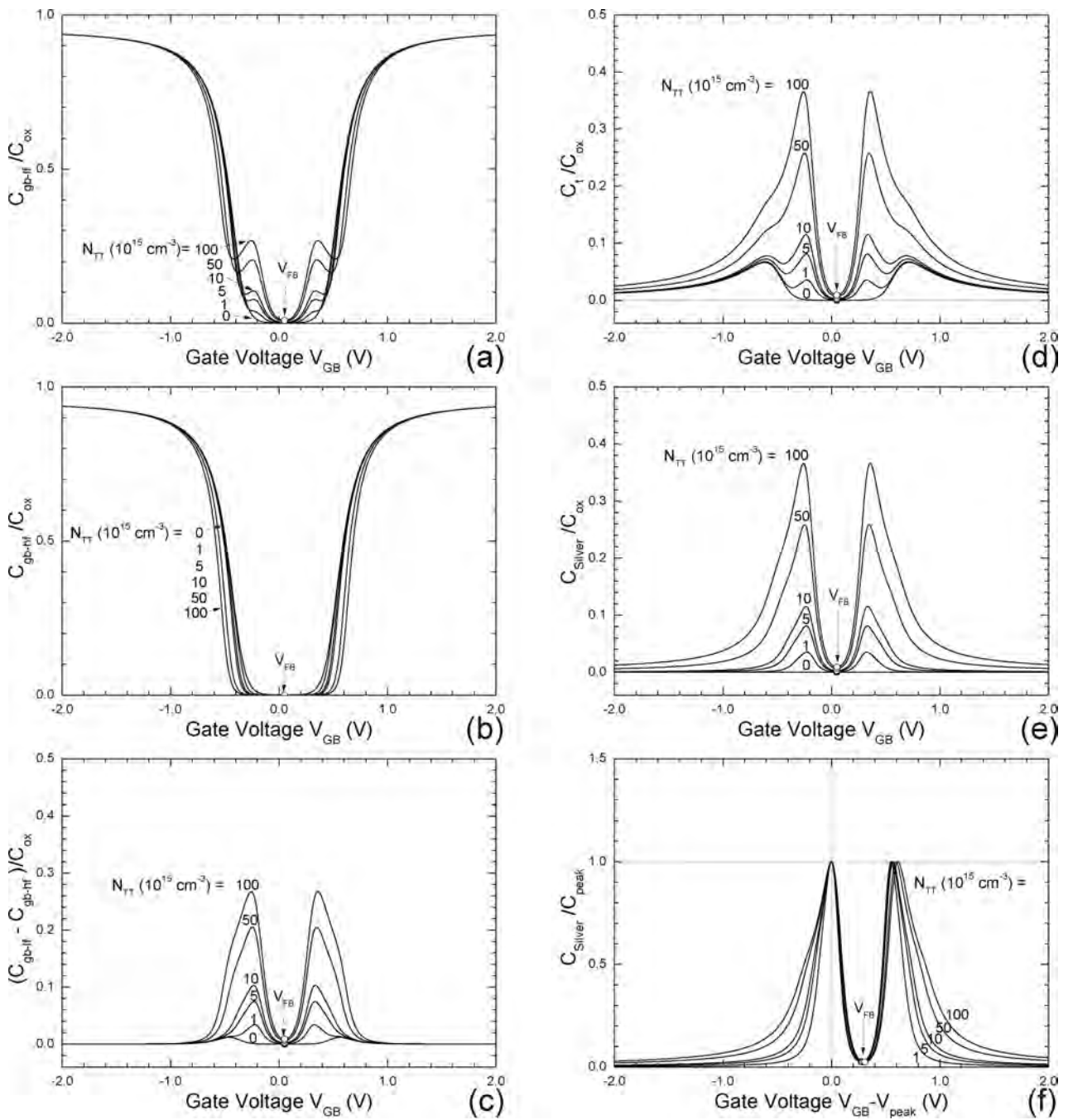
Fig. 16. Capacitance–Voltage curves of compensated Si MOSCs containing a <u>model</u> Gold, a substitutional amphoteric 1-electron and 1-hole trap. $X_{ox} = 3.5$ nm. $T = 300$ K. $P_{AA} = N_{DD} = 120 \times 10^{15}$ cm^{-3}. $E_C - E_D = E_A - E_V = 50$ meV. $g_D = 2$. $g_A = 4$. $N_{TT} = (0, 1, 5, 10, 50, 120) \times 10^{15}$ Au/cm^3. $E_{Gold-1hole} - E_V = 350$ meV. $g_{Gold-1hole} = 1$. $E_C - E_{Gold-1electron} = 550$ meV. $g_{Gold-1electron} = 3$. (a) C_{gb-lf}. (b) C_{gb-hf}. (c) $C_{gb-lf} - C_{gb-hf}$. (d) C_t. (e) C_{Gold}. (f) Normalized-Shifted C_{Gold}.

Fig. 17. Capacitance–Voltage curves of 100% compensated model Si MOSCs containing a model Silver, a substitutional amphoteric 1-electron and 1-hole trap. $X_{ox} = 3.5$ nm. $T = 300$ K. $E_{Si\text{-}gap} = 1200$ meV. $N_C = N_V = 2.50 \times 10^{19}$ cm^{-3}. $P_{AA} = N_{DD} = 100 \times 10^{15}$ cm^{-3}. $E_C - E_D = E_A - E_V = 50$ meV. $g_D = g_A = 2$. $N_{TT} = (0, 1, 5, 10, 50, 100) \times 10^{15}$ Ag/cm^3. $E_{Silver\text{-}1hole} - E_V = E_C - E_{Silver\text{-}1electron} = 350$ meV. $g_{Silver\text{-}1hole} = g_{Silver\text{-}1electron} = 2$. (a) $C_{gb\text{-}lf}$. (b) $C_{gb\text{-}hf}$. (c) $C_{gb\text{-}lf} - C_{gb\text{-}hf}$. (d) C_t. (e) C_{Silver}. (f) Normalized-Shifted C_{Silver}.
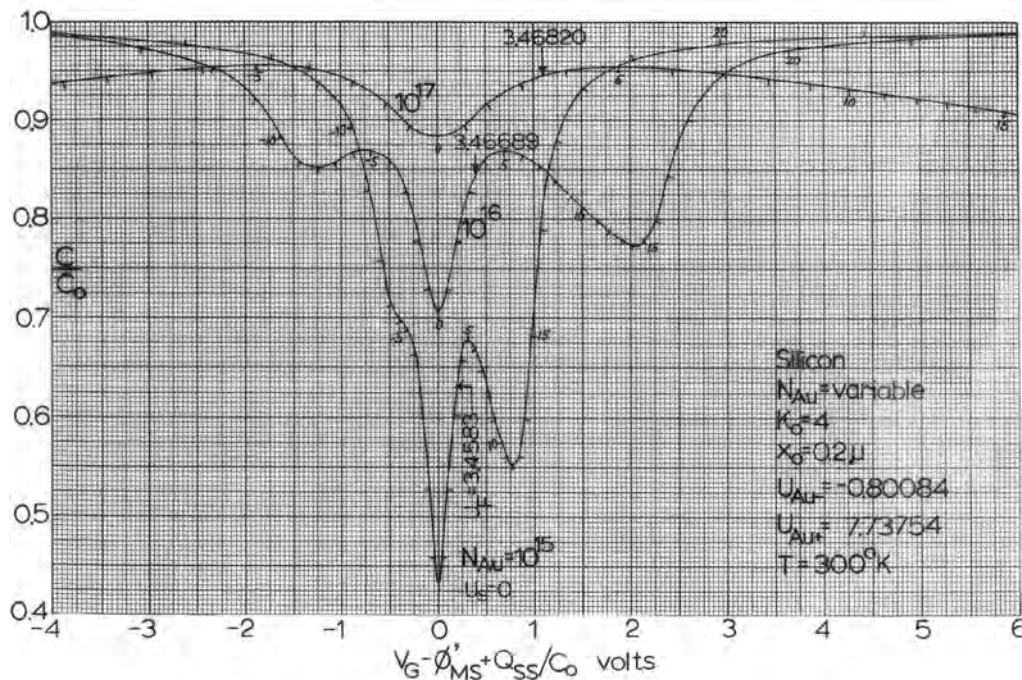
Fig.16.1.20 The low frequency capacitance voltage characteristics of a gold doped silicon which has two energy levels in the band gap.

Fig. 18. Low-frequency Capacitance–Voltage curves of undoped-Si MOS capacitors containing Gold, an amphoteric 1-electron and 1-hole trap. Computed by the senior author using the three slide rules shown in Ref. [2] during 1961–1964 and reported as Fig. 16.1.20 on page 67 of the 1964 report[1]. The $N_{TT} = 10^{16}$ and 10^{17} Au/cm^3 CV curves are identical to the corresponding two CV curves in Fig. 10(a) of this 2011 calculation using a Lenovo T60 personal computer and 64-bit Intel Fortran and IMSL, except the voltage scale due to the difference in oxide thickness, 0.2 μm or 200 nm in 1961 and 3.5 nm in 2011.